

Chlorosphaerolactylates A-D: the natural
chlorinated lactylates isolated from the Portuguese
cyanobacterium *Sphaerospermopsis* sp. LEGE
00249

AUTHOR NAMES

Ignacio Gutiérrez-del-Río^{‡,O}, Nelly Brugerolle de Fraissinette^{†,O}, Raquel Castelo-Branco^{†,O},
Flavio Oliveira[†], João Morais[†], Saúl Redondo-Blanco[‡], Claudio J. Villar[‡], María José
Iglesias[§], Raquel Soengas[§], Virginio Cepas[⊥], Yuly López Cubillos[⊥], Giacomo Sampietro^{||},
Liliana Rodolft^{||}, Felipe Lombó[‡], Sara M. Soto González[⊥], Fernando López Ortiz^{§,*}, Vitor
Vasconcelos^{†,∇}, Mariana A. Reis^{†,*}

AUTHOR ADDRESS

[†] Interdisciplinary Centre of Marine and Environmental Research (CIIMAR/CIMAR),
Terminal de Cruzeiros do Porto de Leixões, University of Porto, 4450-208 Matosinhos,
Portugal

[∇] Faculdade de Ciências, Universidade do Porto, Rua do Campo Alegre, Edifício FC4, 4169-
007 Porto, Portugal

[‡] Universidad de Oviedo (Área de Microbiología, Departamento de Biología Funcional),
IUOPA (Instituto Universitario de Oncología del Principado de Asturias), IISPA (Instituto de

- 20 Investigación Sanitaria del Principado de Asturias), Research Unit “Biotechnology in
21 Nutraceuticals and Bioactive Compounds-BIONUC”. Oviedo, Spain
- 22 § Área de Química Orgánica, Research Centre CIAIMBITAL, Universidad de Almería, Ctra.
23 Sacramento s/n, 04120, Almería, Spain.
- 24 ⊥ ISGlobal, Hospital Clínic—Universitat de Barcelona, 08036 Barcelona, Spain
- 25 || Fotosintetica & Microbiologica S.r.l., Via dei Della Robbia 54, 50132 Firenze, Italy
- 26

27 ABSTRACT

28 The unprecedented natural chlorinated lactylates, chlorosphaerolactylates A-D (**1-4**), were
29 isolated from the methanolic extract of the cyanobacterium *Sphaerospermopsis* sp. LEGE
30 00249 through a combination of bioassay-guided and MS-guided approaches. Compounds **1-4**
31 are esters of (mono-, di- or tri-)chlorinated lauric acid and lactic acid, whose structures were
32 assigned on the basis of spectrometric and spectroscopic methods inclusive of 1D and 2D NMR
33 experiments. High-resolution mass-spectrometry datasets also demonstrated the existence of
34 other minor components that were identified as chlorosphaero(bis)lactylate analogues. The
35 chlorosphaerolactylates were tested for potential antibacterial, antifungal and antibiofilm
36 properties using bacterial and fungal clinical isolates. Compounds **1-4** inhibited the growth of
37 *Staphylococcus aureus* S54F9 and *Candida parapsilosis* SMI416, as well as, affected the
38 biofilm formation of coagulase-negative *Staphylococcus hominis* FI31.

Introduction

In the past few decades, cyanobacteria have been considered as one of the most promising groups of bacteria for natural products discovery.^{1,2} Owing to the distinct ecological niches that these organisms occupy and their particular ecophysiology, the natural products synthesized by cyanobacteria are diverse and structurally unique.³ These metabolites could be peptides, polyketides, derivatives of fatty acids and hybrids thereof, many featuring unusual modifications such as halogenation.⁴ More than 4000 halogenated compounds have been isolated from natural sources including bacteria, fungi, algae, higher plants, invertebrates and vertebrates from distinct environments.^{5,6} Furthermore, the presence of halogen substituents (such as chlorine, bromine and more rarely iodine and fluorine) in natural products influences their biological activity,⁷ representing a valuable and expanding class of natural products. In the last decades, several halogenated fatty acids amide derivatives were isolated from marine cyanobacteria including the malyngamides,⁸ the jamaicamides,⁹ the grenadamides,¹⁰ and the columbamides.¹¹ These compounds have been associated with biological activities such as cytotoxicity, calcium and sodium channel modulation and cannabinoid receptor binding. Additional examples of halogenated fatty acids incorporated in natural peptides can be found in the literature, such as the puwainaphycins originating from a terrestrial cyanobacterium¹² or lyngbyabellin extracted from the marine cyanobacterium *Lyngbya majuscula*.¹³ Moreover, the unusual and fascinating class of chlorosulfolipids was reported in a *Nostoc* sp. strain¹⁴ and more recently aranazoles, extensively polychlorinated compounds were described in a *Fischerella* sp. strain,¹⁵ proving once again the wide structural diversity of halogenated metabolites that cyanobacteria are capable to produce.

Our current interest in identifying novel cyanobacterial metabolites with antibiotic and antibiofilm activity in the framework of the NoMorFilm project¹⁶ led us to investigate the chemical diversity of strains from our in-house cyanobacteria Culture Collection (Blue

Biotechnology and Ecotoxicology Culture Collection – LEGE CC). Through a bioassay-guided approach, *Sphaerospermopsis* sp. LEGE 00249 was pinpointed as a promising producer of antibiofilm and antibacterial metabolites. This cyanobacterial strain was isolated from a Portuguese freshwater reservoir and was previously reported as producer of a prenylated cyanobactin, a cyclic peptide produced by ribosomal synthesis.¹⁷ Herein, we describe the detection, isolation, structural elucidation and bioactivity of four novel chlorinated fatty acid lactylates of cyanobacterial origin, the chlorosphaerolactylates A – D (**1-4**). Moreover, detection of masses correspondent to compounds of the chlorosphaerolactylate type or chlorosphaerobislactylate type are also reported.

Results and discussion

We have recently reported a preliminary screening concerning inhibition of microbial biofilm formation by cyanobacterial organic extracts.¹⁶ As a result, the methanolic extract of the strain *Sphaerospermopsis* sp. LEGE 00249 was selected as promising for isolation of active compounds. In this way, this cyanobacterial strain was regrown (50 L laboratory scale) and its biomass was sequentially extracted with hexane, ethyl acetate and methanol, and the later was submitted to bioassay-guided fractionation, assisted by HPLC, on the basis of the growth inhibition of the clinical isolate *Staphylococcus aureus* S54F9¹⁸ (Supporting Information (SI), Figure S18). Analysis of the active fractions by HRESIMS yielded six groups (G1-G6; Figure 1) that were defined according to their chemical composition. The presence of differential mass peaks showing typical chlorine isotope patterns, indicated the fractions to contain compounds bearing one, two or three chlorine atoms (SI; Figure S19). More specifically, group G2 presented the isotope pattern at m/z 339/341/343 (100:69.9:11 ratio) consistent with the presence of two chlorine atoms in the molecule (m/z 339.1117 [M-H]⁻; C₁₅H₂₆Cl₂O₄) and group G3 showed the isotope cluster at m/z 373/375/377/379 (100:92.8:30.9:3.5 ratio) indicating the

molecule to bear three chlorine substituents (m/z 373.0707 [M-H]⁻; C₁₅H₂₅Cl₃O₄). Furthermore, groups G4 and G5 showed the isotope pattern at m/z 305/307 (100:32.7 ratio) consistent with the presence of only one chlorine atom (m/z 305.1504 [M-H]⁻ and m/z 305.1509 [M-H]⁻, respectively; C₁₅H₂₇ClO₄). Although G4 and G5 showed to have peaks with the same mass, these presented different retention times (SI; Figure S19), suggesting these molecules to be structural isomers. Finally, the chlorine isotopic patterns in groups G1 and G6 presented low intensity (close to the baseline) and were not suitable for NMR experiments.

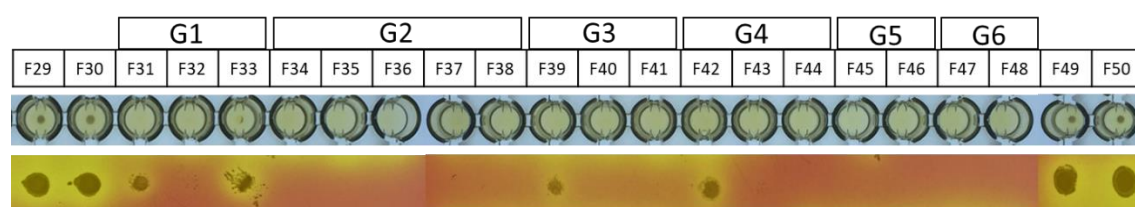


Figure 1. Bioassay-guided discovery of antibacterial compounds. Schematic representation of the 96-well plate showing the active fractions (F31-F48) that inhibited the growth of *S. aureus* S54F9 (clinical isolate). The groups G1-G6 were defined according to their chemical composition.

The structure of compounds **1-4** (Figure 2) was elucidated through the combination of spectroscopic and spectrometric methods. They were identified as esters of chlorinated lauric acid and lactic acid. Nevertheless, the amounts isolated from the 50 L culture were not enough to establish an unambiguous structural elucidation of compound **4** neither for the evaluation of the antibiofilm activity, and thus, the cyanobacterial strain was regrown using Green Wall Panel (GWP®-III) outdoor photobioreactors. The compounds **1-4** were then isolated from this biomass guided by mass spectrometry, though compounds **2** and **3** were not possible to purify and were always isolated as a mixture.

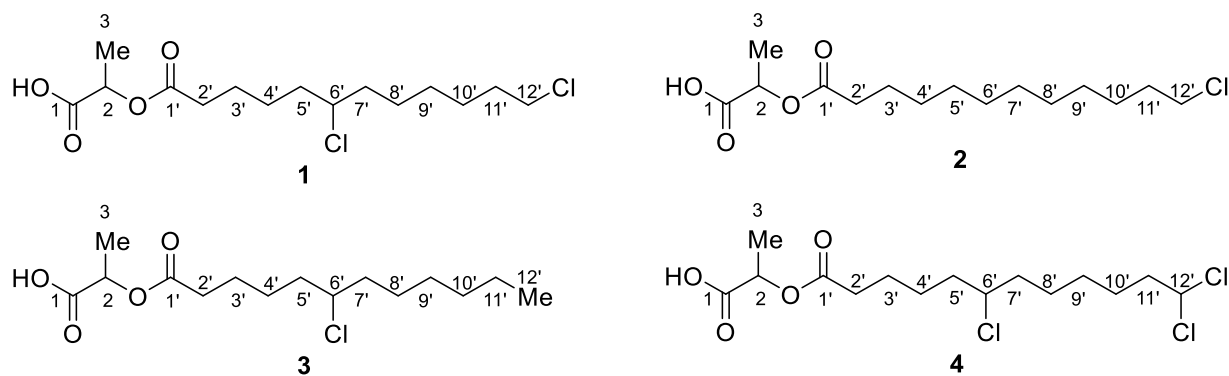
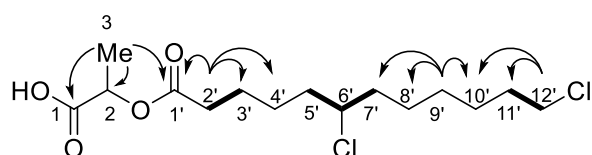


Figure 2. Planar structures of chlorosphaerolactylates A – D (**1-4**).

Compound **1**, named as chlorosphaerolactylate A was obtained as a light-green oil ($[\alpha]_D^{24} +34.1$). The molecular formula $C_{15}H_{26}Cl_2O_4$, consistent with two degrees of unsaturation, was deduced from the HRESIMS spectrum showing the deprotonated molecule mass peak at m/z 339.1117 $[M - H]^-$ (calcd for $C_{15}H_{25}Cl_2O_4$, 339.1135). The IR spectra showed a broad absorption band in the range 3019-2797 cm^{-1} (v-shaped) along with absorptions at 1736 and 1725 cm^{-1} suggesting the presence of two O=C-OR moieties, one of them being a carboxyl functional group (R = H). These findings were corroborated by the ^{13}C NMR signals at δ 175.1 (broad) and 174.7 ppm and account for the two degrees of unsaturation. The 2D HSQC-edited spectrum showed that the remaining thirteen carbon atoms consisted of one CH_3 , ten CH_2 and two CH (Table 1). The structural assignment was based on the analysis of the correlations observed in the 2D HMBC, HSQC-edited and COSY NMR spectra. The methine C2, C6' and methylene carbons C2', C12' were easily identified on chemical shift grounds. Key connections deduced from the HMBC and COSY spectra used to establish the connectivity along the carbon skeleton are shown in Figure 3. Starting with the HMBC spectrum, the doublet at δ 1.46 ($J = 7.2$ Hz) ppm of the methyl group H3 showed three correlations with the methine carbon C2 at δ 70.3 ppm and with the two carbonyl carbons C1/C1' at δ 175.1/174.7 ppm. The correlation of the methylene protons H2' (multiplet, δ 2.4 ppm) with the most shielded signal

indicated that it belongs to C1' (δ 174.7 ppm). H2' also correlated with C3' (δ 25.4 ppm) and C4' (δ 27.0 ppm). The distinction between the two carbons was achieved through the identification of H3' (m, δ 1.65 ppm) via its COSY correlation with H2' and the subsequent HSQC correlation of H3' with the carbon atom to which it is directly bonded. The same strategy was applied to assign the three methylene groups at the other end of the molecule. The triplet at δ 3.56 (J = 6.7 Hz) ppm resulting from the protons H12' correlated with C10' (δ 27.8 ppm) and C11' (δ 33.7 ppm) in the HMBC spectrum. The latter was assigned based on the H12', H11' (m, δ 1.77 ppm) and H11', C11' correlations observed in the COSY and HSQC spectra, respectively. The carbons at position C10' and C11' also showed correlation with the diastereotopic protons H9a'/H9b' (m, δ 1.35 and 1.37 ppm) which in turn correlated with two additional carbon atoms at δ 27.4 and 39.5 ppm. They must correspond to C8' and C7', respectively. This assignment was supported by the COSY correlations of H6' (m, δ 3.93 ppm) with H5a'/H7a' and H5b'/H7b' (m, δ 1.77 and 1.69 ppm). Once the carbon skeleton was assigned, the correlations observed in the HSQC spectrum provided the identification of the protons attached to each carbon atom (Table 1).



— COSY

→ HMBC

Figure 3. Key COSY and HMBC correlations of chlorosphaerolactylate A (**1**)

149 **Table 1.** ^1H NMR (600.13 MHz) and ^{13}C NMR (150.9 MHz) spectroscopic data (δ in ppm, J
150 in Hz) for compounds **1-4**.

	chlorosphaerolactylate		chlorosphaerolactylate		chlorosphaerolactylate		chlorosphaerolactylate	
	A (1)		B (2)		C (3)		D (4)	
position	δ_{H} (J)	δ_{C}	δ_{H} (J)	δ_{C}	δ_{H} (J)	δ_{C}	δ_{H} (J)	δ_{C}
1		175.1 (b) ^a		176.5 (b) ^a		175.6 (b) ^a		178.7 (b) ^a
2	4.99, q (7.2)	70.3	4.99, q (7.1)	71.2	4.99, q (7.1)	70.6	4.91, q (7.1)	72.7
3	1.46, d (7.2)	17.4	1.44, d (7.1)	17.7	1.45, d (7.1)	17.6	1.42, d (7.1)	18.2
1'		174.7		175.1		174.7		175.1
2'	2.40, m	34.6	2.37, m	34.9	2.41, m	34.7	2.4, m	34.9
3'	1.65, m	25.4	1.62, m	25.9	1.64, m 1.67, m	25.4	1.64, m	25.4
4'	1.48, m 1.59, m	27.0	1.35, m	30.2	1.49, m 1.59, m	27.0	1.47, m 1.57, m	27.1
5' b a	1.69, m 1.77, m	39.3	1.33, m	30.4	1.68, m 1.78, m	39.3	1.69, m 1.78, m	39.3
6'	3.93, m	64.8	1.32, m	30.5 (1C) ^b 30.6 (2C) ^b	3.92, m	64.9	3.94, m	64.8
7' b a	1.69, m 1.77, m	39.5	1.32, m		1.66, m 1.76, m	39.7	1.69, m 1.78, m	39.4
8' b a	1.48, m 1.56, m	27.4	1.32, m		1.32, m	30.0	1.45, m 1.56, m	27.3
9' b a	1.35, m 1.37, m	29.5	1.34, m		1.42, m 1.53, m	27.54	1.38, m	29.1
10'	1.46, m	27.8	1.44, m	27.9	1.30, m	32.9	1.57, m	26.9
11'	1.77, m	33.7	1.75, m	33.8	1.33, m	23.6	2.19, m	44.7

12'	3.56, t (6.7)	45.7	3.55, t (6.6)	45.7	0.91, t (7.0)	14.4	5.99, t (6.1)	75.0
------------	------------------	------	------------------	------	------------------	------	------------------	------

^a Broad signal. ^b Could not be assigned unambiguously. All spectra recorded in CD₃OD.

An analogous assignment strategy was applied to the elucidation of the structures of compounds **2**, **3** and **4** (Table 1). They showed the same molecular skeleton than compound **1** only differing in the number and/or position of the chlorine atoms bound to the lauryl moiety. Chlorosphaerolactylate B (**2**) and chlorosphaerolactylate C (**3**) were isolated as light-yellow oils. They are positional isomers of molecular formula C₁₅H₂₇ClO₄ with a HRESIMS peak at *m/z* 305.1504/305.1509 [M-H]⁻ for **2/3** (calculated *m/z* = 305.1525). The position of the chlorine atom in each compound was easily determined through the analysis of the 1D and 2D NMR spectroscopic data. For compound **2**, six methylene protons appeared overlapped in the chemical shift range of δ 1.30 – 1.37 ppm. The correlations originating from the well-resolved signals of the methylene groups at positions 2' (H2', δ 2.37 ppm, m; C2' δ 34.9 ppm) and 12' (H12', δ 3.55 ppm, t, *J* 6.6 Hz; C12' δ 45.7 ppm) provided the connectivity along the fragments C2'-C5' and C12'-C9', respectively. However, the overlap of signals in the ¹H and ¹³C NMR spectra of the methylene groups 6' to 8' prevented their unequivocal assignment. As in compound **1**, the distinguishing feature of the chlorine substituent at C6' (H6', δ 3.92 ppm, m; C6' δ 64.9 ppm) of compound **3** allowed for the proper assignment of the neighboring methylene groups (H5', δ 1.68 ppm, m; C5' δ 39.3 ppm; H7' δ 1.66 ppm, m; C7' δ 39.7 ppm). Compound **4** (chlorosphaerolactylate D) consisted of a light-green oil. The HRESIMS spectrum showed a peak at *m/z* = 373.0707 [M-H]⁻ consistent with a molecular formula of C₁₅H₂₅Cl₃O₄ (calculated *m/z* = 373.0740 for [M-H]⁻). Two of the three chlorine atoms are bound to the terminal carbon of the lauric acid chain as evidenced by the ¹H (H12', δ 5.99 ppm, t, *J* 6.1 Hz) and ¹³C (C12' δ 75.0 ppm) chemical shifts of the methine group C12'. The location of the third chlorine atom at C6' (H6', δ 3.94 ppm, m; C6' δ 64.8 ppm) was achieved through

the observation in the HMBC and COSY NMR spectra of the same set of correlations with neighboring protons as those described above for compound **1** (Figure 3).

The stereocenters at C2 for compounds **1-4** and at C6' for compounds **1** and **3** remain with its configuration unknown at present. Further biosynthetic investigations or synthetic studies will be key to ascertain this point.

Besides the particularity of halogenation found in these novel metabolites, they relate closely to lactylates, which are widely used as emulsifying agents in food and cosmetic industries. In general, lactylates are considered to have non-toxic effects to humans, as well as, biodegradable properties, making them very interesting for industrial applications.¹⁹⁻²² Given the biotechnological potential of our findings, attention was directed to the minor components of fractions F31-F48 (Figure 1). Thus, further HRESIMS analysis pinpointed for the putative existence of other novel mono-, di-, and tri-chlorinated fatty acid lactylate-like compounds (Table 2). The presence of other novel positional isomers of compounds **1-4** was suggested through the detection of the same *m/z* but at different retention times (SI; Figure S23-S26). Moreover, detailed analysis of the ions generated by the in-source fragmentation pointed to compounds bearing one more unit of lactic acid, the mono-, di-, and tri-chlorinated bislactylates (Figure 4; Table 2). To confirm these observations, in-source fragmentation of a commercial standard of sodium lauroyl lactylate containing a mixture of 23:9:1.33 2-(dodecanoyloxy)propanoic acid (C₁₅H₂₈O₄), 2-((2-(dodecanoyloxy)propanoyl)oxy)propanoic acid (C₁₈H₃₂O₆) and 2-((2-((2-(dodecanoyloxy)propanoyl)oxy)propanoyl)oxy)propanoic acid (C₂₁H₃₆O₈) acid was also investigated. The in-source-formed species evidenced the expected loss of C₃H₄O₂ corroborating the same fragmentation pattern as observed for the chlorosphaerobislactylates (SI, Figures S20-S22).

Table 2. HRESIMS-based detection of putative chlorinated fatty acid lactylates in fractions F31-F49.

<i>m/z</i> [M-H] ⁻	Proposed Molecular Formula	Analytical Error (mmu)	
Mono- chlorinated compounds			Difference to compounds 2 and 3
305.1504	C ₁₅ H ₂₇ ClO ₄	0.0020	Putative positional isomer
377.1707	C ₁₈ H ₃₁ ClO ₆	0.0029	+ C ₃ H ₄ O ₂ (putative bis-lactylate); positional isomers
377.1697	C ₁₈ H ₃₁ ClO ₆	0.0039	
377.1702	C ₁₈ H ₃₁ ClO ₆	0.0034	
Di- chlorinated compounds			Difference to compound 1
339.1105	C ₁₅ H ₂₆ Cl ₂ O ₄	0.0030	Putative positional isomer
339.1107	C ₁₅ H ₂₆ Cl ₂ O ₄	0.0028	
339.1105	C ₁₅ H ₂₆ Cl ₂ O ₄	0.0030	
339.1103	C ₁₅ H ₂₆ Cl ₂ O ₄	0.0032	
411.1300	C ₁₈ H ₃₀ Cl ₂ O ₆	0.0046	+ C ₃ H ₄ O ₂ (putative bis-lactylate)
Tri- chlorinated compounds			Difference to compound 4
373.0713	C ₁₅ H ₂₅ Cl ₃ O ₄	0.0032	Putative positional isomer
445.0906	C ₁₈ H ₂₉ Cl ₃ O ₆	0.0050	+ C ₃ H ₄ O ₂ (putative bis-lactylate)

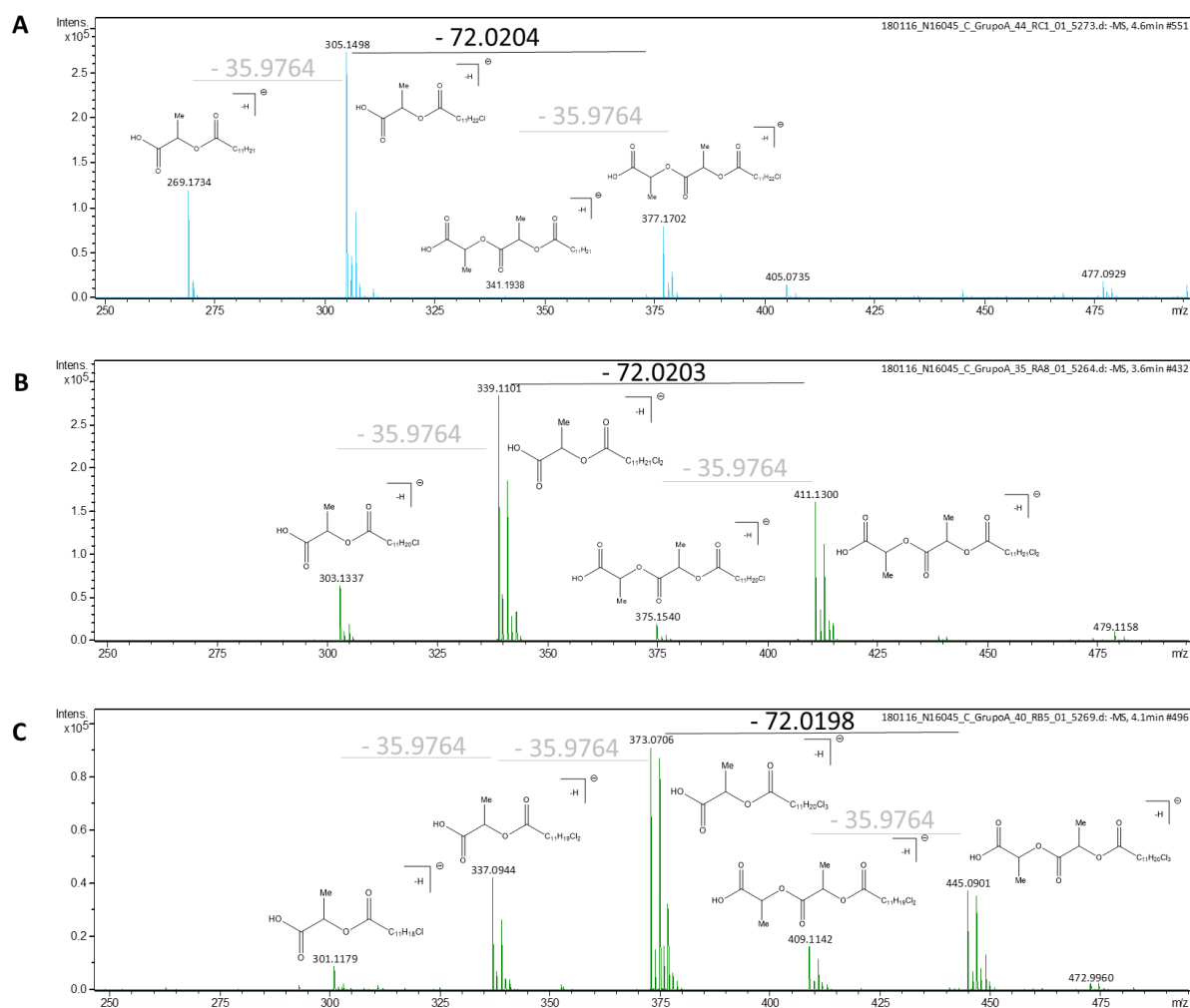


Figure 4. Mass spectra of the putative mono- (A), di- (B), and tri- (C) chlorinated bislactylates.

Since the position of the chlorine atoms could not be ascertained, in order to rationalize the analysis of the ions generated by the in-source fragmentation, the chlorinated moiety is represented by its molecular formula. Mass differences are shown in grey and black color. The loss of chlorine atoms is also confirmed by change in the isotope pattern.

The chlorosphaerolactylates A-D were isolated on the basis of an antibacterial screening. Thus, compounds **1** and **4** as well as mixture of compounds **2/3** (51:33 ratio) were tested for antibacterial and antifungal activities using resistant strains driven from clinical isolates: *Escherichia coli* AR, *S. aureus* S54F9¹⁸, and *Candida parapsilosis* SMI416²³ (Table 3). The chlorosphaerolactylates inhibited the growth of *S. aureus* and *C. parapsilosis* in the range of

concentrations between 1024-2048 µg/mL. No antibacterial effect was observed against the clinical isolate *E. coli*.

Table 3. Antibacterial, antifungal and antibiofilm activities of compounds **1-4**.

Compound	Antibacterial /Antifungal activity			Antibiofilm activity
	MBC ^a /MFC ^b (µg/mL)			MBIC ₅₀ ^c (µg/mL)
	<i>E. coli</i>	<i>S. aureus</i>	<i>C. parapsilosis</i>	Coagulase-negative <i>S. hominis</i> FI31
1	NI	2048	1024	200
2/3 (51:33)	NI	1024	1024	313
4	NI	1024	2048	430

^aMBC: minimum bactericidal concentration; ^bMFC: minimum fungicidal concentration;

^cMBIC₅₀: minimum concentration of the test compound that resulted in ≥ 50% inhibition of biofilm formation. NI: no inhibition at the highest tested concentration (2048 µg/mL)

Moreover, antibiofilm activity was assessed against coagulase-negative *S. hominis* FI31 (Table 3), a clinical isolate collected from an infected prosthesis. The compounds **1**, **2/3** and **4** were able to reduce the biofilm formation showing a 3 fold-decrease in optical density (OD) in comparison with the OD obtained for the positive control, with MBIC₅₀ values of 200, 313 and 430 µg/mL, respectively.

Concerning the antibacterial effects of lactylates, most of what is found in the literature derives from patents. For instance, the patent document WO2018222184A1²⁴ refers to antimicrobial compositions, which include an acyl lactylate, for inhibiting microbial growth in personal care products. Likewise, compositions with fatty acid esters as the predominant component were

subject of the US6878757B2²⁵ patent as an antimicrobial coating for absorbable surgical materials. Furthermore, the patent document US7973006B2²⁶ describes the use of an antibacterial agent (composed of mono- and/or di-lactylate esters of octanoic acid, or decanoic acid, or dodecanoic acid, or tetradecanoic acid, or palmitic acid, or oleic acid) against gram-negative bacteria (*E. coli*, *Salmonella* sp., *Pseudomonas* sp. or *Campylobacter* sp.).

In conclusion, this study describes the structure of four novel chlorosphaerolactylates, isolated from the cyanobacterium *Sphaerospermopsis* sp. LEGE 00249, with antibiofilm and antibacterial and antifungal properties. In addition, other putative chlorosphaero(bis)lactylates were also reported for the first time. These findings taken together, add to the knowledge of the fascinating world of cyanobacterial secondary metabolites, namely to the class of halogenated fatty acid derivatives.

Experimental section

Cyanobacterial strain and culture conditions. The cyanobacterium strain *Sphaerospermopsis* sp. LEGE 00249 was obtained from the LEGE CC²⁷. The detection of compounds was performed using biomass of cultures grown in laboratory conditions. The strain was cultured up to 50 L in Z8 medium²⁸ at 25 °C, with constant aeration with a photoperiod of 14 h/10 h light and dark respectively, and at light intensity of 10-30 $\mu\text{mol photons s}^{-1}.\text{m}^{-2}$. At the exponential phase, cells were harvested through centrifugation, then frozen and freeze-dried. In order to obtain larger amount of biomass from *Sphaerospermopsis* sp. LEGE 00249, that could allow the isolation and chemical characterization of compounds **1-4**, the culture was scaled-up in outdoor conditions. In this context, the strain was cultivated

in a modified BG11 medium²⁹, in which nutrients were added according to growth, and gradually adapted to outdoor conditions in particular with regards to light intensity and photoperiod using as culture vessel a 7-L bubbled tube placed outdoors. A volume containing 15 g of dry biomass was then transferred to a 40-L Green Wall Panel (GWP®-III) photobioreactor³⁰ in order to start with an initial biomass concentration of 20 g.m⁻² of reactor illuminated surface. For the first days, the photobioreactor was tilted backward (North facing) to reduce the light intercepted and thus reduce light stress to the culture, then it was tilted (50°) facing South to increase light availability and thus maximize growth and productivity. The culture was kept at a maximum temperature of 28 °C by circulating cold water inside a stainless-steel serpentine placed within the culture chamber and it was bubbled with air at a flow rate of 0.3 L.L⁻¹ min⁻¹. Pure CO₂ was injected when the pH value exceeded 7.8. The culture was firstly managed in batch and then in semi-continuous with a 30% daily dilution. In this latter culture regimen biomass productivity was 7.6 g.m⁻² ± 3.0 of reactor's illuminated surface.day⁻¹ with a solar radiation of 29.6 ± 0.3 MJ.m⁻².day⁻¹. The culture was harvested at the steady-state by centrifugation, and the biomass frozen and lyophilized prior to be used for the following experiments.

Bacterial strains and culture conditions. *E. coli* clinical isolate (AR-collected from urine at the Hospital Clinic of Barcelona), *S. aureus spa* type t1333 (S54F9)¹⁸ and *C. parapsilosis* clinical isolate from bloodstream infection (SMI416)²³ were employed for antibacterial and antifungal activities. *E. coli*, *S. aureus* and *C. parapsilosis* were resuscitated on MH agar (Mueller-Hinton Agar, Oxoid) at 37 °C from 25 % glycerol (v/v) stocks kept at -20 °C, and maintained thereafter at 4 °C. Coagulase-negative *S. hominis* FI31 is a clinical isolated collected from an infected prosthesis at the Hospital Clinic of Barcelona. Bacterial culture

media were purchased from ThermoScientific. All other solutions and media were made with ultrapure deionized water and were sterilized by autoclaving at 121 °C for 15 min.

Antibiotic assays. The antimicrobial properties of the three crude extracts (hexane, ethyl acetate and methanol), the fractions obtained in the different purification steps, as well as of the isolated compounds **1-4**, were tested via microdilution assay following the guidelines of the two established organizations and committees, the CLSI³¹ and EUCAST³². MBC/MFC (Minimum Bactericidal/Fungicidal Concentration) was determined according to CLSI protocol by plating 20 µL from each well showing no visible growth at 24 h onto a solid medium. The lowest concentration of the compound that killed > 99.9% of the initial inoculum was determined to be the MBC/MFC. The antibiotic activity of the extracts and molecules was determined using 96-well U-bottom microtiter plates (ThermoScientific). Microorganisms were grown overnight (37 °C, 250 rpm) and diluted in MHB (Mueller-Hinton Broth, Oxoid) up to the desired cell density. When crude extracts and HPLC fractions were tested for bioactivity-guided fractionation purposes, no serial dilutions were performed (yes/no method) and only for compounds **1-4** two-fold dilutions were carried out in order to obtain a MBC/MFC value. Both protocols are described below. In order to perform antibiotic susceptibility tests of crude extracts and HPLC fractions, 50 µL of each HPLC fraction or crude extract resuspended in 14% MeOH in water (v/v) were mixed with 50 µL of the *S. aureus* S54F9 suspension at 10⁶ CFU/mL in 2x MHB in a microtiter plate and incubated statically overnight at 37 °C (final desired inoculum = 5.10⁵ CFU/mL, final concentration of MeOH in bioassay plate = 7% (v/v), final volume per well = 100 µL). Growth controls (broth with bacterial inoculum, no bioactive molecule) as well as sterility (broth only) and solvent controls (bacterial inoculum with a final concentration of 7% MeOH in water v/v) were included.³³ Microbial sedimentation was checked by visual verification and each experiment was performed in duplicate. The microtiter plate was replicated onto a selective/differential solid medium such as Mannitol Salt Agar

(SMA, VWR Chemicals) with a 96-pin replicator in order to distinguish between bacteriostatic and bactericidal activities.

When compounds **1-4** were tested for antibiotic activity, stock solutions in MeOH 28% (v/v) were prepared at a concentration of 8192 µg/mL which resulted in a final concentration in the first dilution well of 1024 µg/mL. 50 µL of water were added to each well except to the solvent control (bacterial inoculum with a final concentration of 7% MeOH in water v/v) and 50 µL of each compound (per duplicate) were added to the first well of each row and two-fold serial dilutions were performed transferring 50 µL to the following well. Finally, 50 µL of each microorganism at 10⁶ CFU/mL (*S. aureus* and *E. coli*) in 2 x MHB were added (final concentration of MeOH in bioassay plate = 7%, final volume per well = 100 µL); in the case of *C. parapsilosis*, the cells concentration was 5·10⁵ CFU/mL. Growth and sterility controls were included as well. The microtiter plate was replicated onto a selective/differential solid medium depending on each microorganism: Eosin Methylene Blue Agar for *E. coli* (EMB, Merck Chemicals), Mannitol Salt Agar for *S. aureus* (SMA, VWR Chemicals) and Sabouraud Dextrose Agar for *C. parapsilosis* (VWR Chemicals).

Antibiofilm assays. The pure compounds were resuspended with 150 µL of DMSO 10% (final concentration 5%). Fifty µL of each extract was added into well and serial diluted with 50 µL of bacterial suspension at a concentration of 10⁶ CFU/mL in TSB culture medium. The plates were incubated for 48 h at 37 °C. The plates were washed with sterile 1X phosphate-buffered saline (PBS) and stained with 200 µL of 0.2 % crystal violet (CV). CV was resuspended using a 3 % glacial acetic acid solution and optical density read in a spectrophotometer at 580 nm. All the experiments were carried out in duplicate. A negative control (culture medium without inoculum) and a positive control (culture medium with inoculum) were included in each plate.

All the plates were covered with adhesive foil lids to avoid evaporation. The MBIC was defined as the lowest concentration of drug that resulted in a three-fold decrease of the optical density of 580 nm (OD₅₈₀) in comparison with the positive growth-control value. The biofilm inhibition rates were calculated using the equation: $100 \times (1 - \text{OD}_{580} \text{ of the test} / \text{OD}_{580} \text{ of non-treated control})$. The MBIC₅₀ was defined as the lowest concentration that caused 50% inhibition on the formation of biofilm.

General chemical experimental procedures. Optical rotation was obtained using a P-2000 polarimeter (JASCO). Infrared spectrum was collected on a Nicolet iS5 FTIR spectrometer (ThermoScientific). The 1D and 2D NMR spectrometric data were measured on a Bruker AV600 spectrometer equipped with a 5 mm ¹H, ¹³C, ¹⁵N, ³¹P cryoprobe working at a ¹H frequency of 600.13 MHz and ¹³C frequency of 150.9 MHz. NMR samples were prepared by dissolving the fraction in 0.5 mL of CD₃OD and transferring the solution to a 5 mm NMR tube. The structural elucidation was based on the analysis of a set of 1D and 2D NMR spectra including ¹H, gNOESY-¹H (water suppression), ¹³C, COSY, HSQC edited and HMBC. The solvent signal was used as internal NMR reference. Standard Bruker software (TopSpin 3.6) was used for the acquisition and processing of the 1D and 2D NMR spectra.

Bioactivity-guided fractionation and LC-MS analysis of the antibacterial fractions. The procedure is supplied in the Supporting Information.

Consecutive isolations of compound 1, 2, 3 and 4. The isolation procedure is supplied in the Supporting Information.

Chlorosphaerolactylate A ([(6,12-dichlorododecanoyl)oxy]propanoic acid) (1): light-green oil; $[\alpha]_D^{24} +33.1$ (c 0.01, MeOH); IR (KBr) ν_{max} 2937, 1736 and 1725 cm⁻¹; ¹H and ¹³C NMR

353 spectroscopic data (CD₃OD), see Table 1; HRMS m/z 339.1117 [M-H]⁻ (calcd for C₁₅H₂₆Cl₂O₄
354 = 339.1135).

355 *Chlorosphaerolactylate B* ([*(12-chlorododecanoyl)oxy*]propanoic acid) (**2**): light-yellow oil;
356 ¹H and ¹³C NMR spectroscopic data (CD₃OD), see Table 1; HRMS m/z 305.1504 [M-H]⁻
357 (calcd for C₁₅H₂₇ClO₄ = 305.1525).

358 *Chlorosphaerolactylate C* ([*(6-chlorododecanoyl)oxy*]propanoic acid) (**3**): light-yellow oil;;
359 ¹H and ¹³C NMR spectroscopic data (CD₃OD), see Table 1; HRMS m/z 305.1509 [M-H]⁻
360 (calcd for C₁₅H₂₇ClO₄ = 305.1525).

361 *Chlorosphaerolactylate D* ([*(6,12,12-trichlorododecanoyl)oxy*]propanoic acid) (**4**): light-
362 green oil; ¹H and ¹³C NMR spectroscopic data (CD₃OD), see Table 1; HRMS m/z 373.0707
363 [M-H]⁻ (calcd for C₁₅H₂₅Cl₃O₄ = 373.0746)

364

365 AUTHOR INFORMATION

366 Corresponding Author

367 * Mariana A. Reis, mreis@ciimar.up.pt, Interdisciplinary Centre of Marine and Environmental
368 Research (CIIMAR/CIMAR), Terminal de Cruzeiros do Porto de Leixões, University of Porto,
369 4450-208 Matosinhos, Portugal

370 * Fernando Lopez Ortiz, flortiz@ual.es, Área de Química Orgánica, Research Centre
371 CIAIMBITAL, Universidad de Almería, Ctra. Sacramento s/n, 04120, Almería, Spain.

372

373 Author Contributions

374 ^o I.G.R., N.B.F. and R.C.B contributed equally to this work sharing the first co-authorship.

I.G.R. and S.R.B. performed the antibiotic assays I.G.R. conducted the bioassay-guided fractionation and the HRESIMS experiments for identification of putative chlorosphaero(bis)lactylates. F.L. and C.J.V supervised the work described for I.G.R. and S.R.B. I.G.R. and F.L. contributed to the writing of the paper. N.B.F., R.C.B and M.A.R isolated compounds **1-4** from large scale biomass, determined the optical rotation of **1** and significantly contributed to the writing of the paper. F.O. and J. M. performed lab scale growth and extractions and V.V. supervised the works described for N.B.F., R.C.B, M.A.R, F.O. and J. M. M.J.I., R.S. and F.L.O. acquired the NMR data, and performed and wrote the structure elucidation of compounds **1-4**. V.C. and Y.L.C. performed the antibiofilm assays under the supervision of S.M.S.G. Large scale cultivation of the cyanobacterium outdoors was conducted by G.S. under L.R. supervision. M.A.R. took the lead in writing and revising the manuscript using the inputs from all the authors. All authors have given approval to the final version of the manuscript.

Acknowledgments

This work was funded by the European Commission under the H2020 program, NoMorFilm Project (Grant Agreement 634588). CIIMAR was additionally supported by the FCT strategic funds UIDB/04423/2020 and UIDP/04423/2020. R.C.B. acknowledges financial support from a Fundação para a Ciência e a Tecnologia (FCT) fellowship SFRH/BD/136367/2018. University of Oviedo also thanks *Programa de Ayudas a Grupos de Investigación del Principado de Asturias* (IDI/2018/000120) and *Programa Severo Ochoa de Ayudas Predoctorales para la investigación y docencia* from Principado de Asturias (grant BP16023 to I.G.R.). HRESIMS experiments were conducted at the Mass spectrometry unit of the University of Oviedo (Servicios Científico-Técnicos). ISGlobal is a CERCA center from the

Generalitat of Catalunya and a Severo Ochoa Center (Spanish Ministry of Science, Innovations and Universities) supported by Planes Nacionales de I+D+i 2008-2011 / 2013-2016 and Instituto de Salud Carlos III, Subdirección General de Redes y Centros de Investigación Cooperativa, Ministerio de Economía y Competitividad, Spanish Network for Research in Infectious Diseases (REIPI RD12/0015/0013 and REIPI RD16/0016/0010) co-financed by European Development Regional Fund "A way to achieve Europe" and operative program Intelligent Growth 2014-2020. The authors acknowledge the support and the use of resources of EMBRC-ERIC, specifically of the Portuguese infrastructure node of the European Marine Biological Resource Centre (EMBRC-PT) CIIMAR – PINFRA/22121/2016 – ALG-01-0145-FEDER-022121, financed by the European Regional Development Fund (ERDF) through COMPETE2020 - Operational Programme for Competitiveness and Internationalisation (POCI) and national funds through FCT/MCTES.

References

- (1) Dittmann, E.; Gugger, M.; Sivonen, K.; Fewer, D. P. Natural Product Biosynthetic Diversity and Comparative Genomics of the Cyanobacteria. *Trends Microbiol.* **2015**, *23* (10), 642–652. <https://doi.org/10.1016/j.tim.2015.07.008>.
- (2) Newman, D. J.; Cragg, G. M. Natural Products as Sources of New Drugs from 1981 to 2014. *J. Nat. Prod.* **2016**, *79* (3), 629–661. <https://doi.org/10.1021/acs.jnatprod.5b01055>.
- (3) Demay, J.; Bernard, C.; Reinhardt, A.; Marie, B. Natural Products from Cyanobacteria: Focus on Beneficial Activities. *Mar. Drugs* **2019**, *17* (6), 1–49. <https://doi.org/10.3390/md17060320>.
- (4) Dembitsky, V. M.; Srebnik, M. Natural Halogenated Fatty Acids: Their Analogues and Derivatives. *Prog. Lipid Res.* **2002**, *41* (4), 315–367. <https://doi.org/10.1016/S0163->

- 424 7827(02)00003-6.
- 425 (5) Gribble, G. W. Natural Organohalogens: A New Frontier for Medicinal Agents? *J.*
426 *Chem. Educ.* **2004**, *81* (10), 1441–1449. <https://doi.org/10.1021/ed081p1441>.
- 427 (6) Atashgahi, S.; Häggblom, M. M.; Smidt, H. Organohalide Respiration in Pristine
428 Environments: Implications for the Natural Halogen Cycle. *Environ. Microbiol.* **2018**,
429 *20* (3), 934–948. <https://doi.org/10.1111/1462-2920.14016>.
- 430 (7) Neumann, C. S.; Fujimori, D. G.; Walsh, C. T. Halogenation Strategies In Natural
431 Product Biosynthesis. *Chem. Biol.* **2008**, *15* (2), 99–109.
432 <https://doi.org/10.1016/j.chembiol.2008.01.006>.
- 433 (8) Kan, Y.; Sakamoto, B.; Fujita, T.; Nagai, H. New Malyngamides from the Hawaiian
434 Cyanobacterium *Lyngbya majuscula*. *J. Nat. Prod.* **2000**, *63* (12), 1599–1602.
435 <https://doi.org/10.1021/np000250t>.
- 436 (9) Edwards, D. J.; Marquez, B. L.; Nogle, L. M.; Mcphail, K.; Goeger, D. E.; Roberts, M.
437 A.; Gerwick, W. H. CNTNAP2 Is Significantly Associated with Schizophrenia and
438 Major Depression in the Han Chinese Population. *Psychiatry Res.* **2012**, *1* (1), 817–
439 833. <https://doi.org/10.1016/j>.
- 440 (10) Jiménez, J. I.; Vansach, T.; Yoshida, W. Y.; Sakamoto, B.; Pörzgen, P.; Horgen, F. D.
441 Halogenated Fatty Acid Amides and Cyclic Depsipeptides from an Eastern Caribbean
442 Collection of the Cyanobacterium *Lyngbya majuscula*. *J. Nat. Prod.* **2009**, *72* (9),
443 1573–1578. <https://doi.org/10.1021/np900173d>.
- 444 (11) Lopez, J. A. V.; Petitbois, J. G.; Vairappan, C. S.; Umezawa, T.; Matsuda, F.; Okino,
445 T. Columbamides D and E: Chlorinated Fatty Acid Amides from the Marine
446 Cyanobacterium *Moorea bouillonii* Collected in Malaysia. *Org. Lett.* **2017**, *19* (16),
447 4231–4234. <https://doi.org/10.1021/acs.orglett.7b01869>.
- 448 (12) Moore, R. E.; Bornemann, V.; Niemczura, W. P.; Gregson, J. M.; Chen, J. L.; Norton,

449 T. R.; Patterson, G. M. L.; Helms, G. L. Puwainaphycin C, a Cardioactive Cyclic
 450 Peptide from the Blue-Green Alga *Anabaena* BQ-16-1. Use of Two-Dimensional
 451 Carbon-13-Carbon-13 and Carbon-13-Nitrogen-15 Correlation Spectroscopy in
 452 Sequencing the Amino Acid Units. *J. Am. Chem. Soc.* **1989**, *111* (16), 6128–6132.
 453 <https://doi.org/10.1021/ja00198a021>.

454 (13) Luesch, H.; Yoshida, W. Y.; Moore, R. E.; Paul, V. J.; Mooberry, S. L. Isolation,
 455 Structure Determination, and Biological Activity of Lyngbyabellin A from the Marine
 456 Cyanobacterium *Lyngbya majuscula*. *J. Nat. Prod.* **2000**, *63* (5), 611–615.
 457 <https://doi.org/10.1021/np990543q>.

458 (14) Mercer, E. I.; Davies, C. L. Chlorosulpholipids in Algae. *Phytochemistry* **1975**, *14* (7),
 459 1545–1548. [https://doi.org/10.1016/0031-9422\(75\)85348-9](https://doi.org/10.1016/0031-9422(75)85348-9).

460 (15) Moosmann, P.; Ueoka, R.; Gugger, M.; Piel, J. Aranazoles: Extensively Chlorinated
 461 Nonribosomal Peptide-Polyketide Hybrids from the Cyanobacterium *Fischerella* sp.
 462 PCC 9339. *Org. Lett.* **2018**, *20* (17), 5238–5241.
 463 <https://doi.org/10.1021/acs.orglett.8b02193>.

464 (16) Cepas, V.; López, Y.; Gabasa, Y.; Martins, C. B.; Ferreira, J. D.; Correia, M. J.;
 465 Santos, L. M. A.; Oliveira, F.; Ramos, V.; Reis, M.; et al. Inhibition of Bacterial and
 466 Fungal Biofilm Formation by 675 Extracts from Microalgae and Cyanobacteria.
 467 *Antibiotics* **2019**, *8* (2), 1–12. <https://doi.org/10.3390/antibiotics8020077>.

468 (17) Martins, J.; Leikoski, N.; Wahlsten, M.; Azevedo, J.; Antunes, J.; Jokela, J.; Sivonen,
 469 K.; Vasconcelos, V.; Fewer, D. P.; Leão, P. N. Sphaerocyclamide, a Prenylated
 470 Cyanobactin from the Cyanobacterium *Sphaerospermopsis* sp. LEGE 00249. *Sci. Rep.*
 471 **2018**, *8* (1), 1–9. <https://doi.org/10.1038/s41598-018-32618-5>.

472 (18) Aalbæk, B.; Jensen, L. K.; Jensen, H. E.; Olsen, J. E.; Christensen, H. Whole-Genome
 473 Sequence of *Staphylococcus aureus* S54F9 Isolated from a Chronic Disseminated

- 474 Porcine Lung Abscess and Used in Human Infection Models. *Genome Announc.* **2015**,
475 3 (5), 9–10. <https://doi.org/10.1128/genomeA.01207-15>.
- 476 (19) Boutte, T.; Skogerson, L. Stearoyl-2-Lactylates and Oleoyl Lactylates. *Emuls. food*
477 *Technol.* **2004**, 206–225.
- 478 (20) Wang, F. C.; Marangoni, A. G. Advances in the Application of Food Emulsifier α -Gel
479 Phases: Saturated Monoglycerides, Polyglycerol Fatty Acid Esters, and Their
480 Derivatives. *J. Colloid Interface Sci.* **2016**, 483, 394–403.
481 <https://doi.org/10.1016/j.jcis.2016.08.012>.
- 482 (21) Shah, R.; Kolanos, R.; DiNovi, M. J.; Mattia, A.; Kaneko, K. J. Dietary Exposures for
483 the Safety Assessment of Seven Emulsifiers Commonly Added to Foods in the United
484 States and Implications for Safety. *Food Addit. Contam. Part A* **2017**, 34 (6), 905–917.
485 <https://doi.org/10.1080/19440049.2017.1311420>.
- 486 (22) Draelos, Z. D.; Donald, A. The Effect of an Anti-Inflammatory Botanical
487 Cleanser/Night Mask Combination on Facial Redness Reduction. *J. Drugs Dermatol.*
488 **2018**, 17 (6), 671–676.
- 489 (23) Pannanusorn, S.; Ramírez-Zavala, B.; Lünsdorf, H.; Agerberth, B.; Morschhäuser, J.;
490 Römling, U. Characterization of Biofilm Formation and the Role of BCR1 in Clinical
491 Isolates of *Candida parapsilosis*. *Eukaryot. Cell* **2014**, 13 (4), 438–451.
492 <https://doi.org/10.1128/EC.00181-13>.
- 493 (24) Jeffery, R.; Paige, N.; Corey, T.; Luke, D. WO2018222184A1: Antimicrobial
494 Composition Including an Acyl Lactylate and a Glycol and Methods of Inhibiting
495 Microbial Growth Utilizing the Same, 2018.
- 496 (25) Roby, M. US6878757B2: Antimicrobial Suture Coating, 2005.
- 497 (26) Ramirez, M.; Kremer, D. R. US7973006B2: Antibacterial Agent Based On Fatty Acid
498 Esters Of Hydroxy Carboxylic Acid Acids, 2011.

- 499 (27) Ramos, V.; Morais, J.; Castelo-Branco, R.; Pinheiro, Â.; Martins, J.; Regueiras, A.;
500 Pereira, A. L.; Lopes, V. R.; Frazão, B.; Gomes, D.; et al. Cyanobacterial Diversity
501 Held in Microbial Biological Resource Centers as a Biotechnological Asset: The Case
502 Study of the Newly Established LEGE Culture Collection. *J. Appl. Phycol.* **2018**, *30*
503 (3), 1437–1451. <https://doi.org/10.1007/s10811-017-1369-y>.
- 504 (28) Kotai, J. Instructions for Preparation of Modified Nutrient Solution Z8 for Algae. *Inst.*
505 *Water Res. Blind.* **1972**.
- 506 (29) Rippka, R. [1] Isolation and Purification of Cyanobacteria. *Methods Enzymol.* **1988**,
507 *167*, 3–27. [https://doi.org/10.1016/0076-6879\(88\)67004-2](https://doi.org/10.1016/0076-6879(88)67004-2).
- 508 (30) Rodolfi, L.; Biondi, N.; Guccione, A.; Bassi, N.; D'Ottavio, M.; Arganaraz, G.;
509 Tredici, M. R. Oil and Eicosapentaenoic Acid Production by the Diatom
510 *Phaeodactylum tricornutum* Cultivated Outdoors in Green Wall Panel (GWP®)
511 Reactors. *Biotechnol. Bioeng.* **2017**, *114* (10), 2204–2210.
512 <https://doi.org/10.1002/bit.26353>.
- 513 (31) Clinical and Laboratory Standards Institute (CLSI). Performance Standards for
514 Antimicrobial Susceptibility Testing. 26th ed. CLSI supplement M100-S26, Wayne,
515 Pennsylvania, USA, **2016**.
- 516 (32) European Society of Clinical Microbiology and Infectious Diseases. Determination of
517 Minimum Inhibitory Concentrations (MICs) of Antibacterial Agents by Broth
518 Dilution. *Clin. Microbiol. Infect.* **2003**, *9* (8), ix–xv. [https://doi.org/10.1046/j.1469-](https://doi.org/10.1046/j.1469-0691.2003.00790.x)
519 [0691.2003.00790.x](https://doi.org/10.1046/j.1469-0691.2003.00790.x).
- 520 (33) Wiegand, I.; Hilpert, K.; Hancock, R. E. W. Agar and Broth Dilution Methods to
521 Determine the Minimal Inhibitory Concentration (MIC) of Antimicrobial Substances.
522 *Nat. Protoc.* **2008**, *3* (2), 163–175. <https://doi.org/10.1038/nprot.2007.521>.

523